Ottens, E. P. K., and E. J. deJong, "A Model for Secondary Nucleation in a Stirred Vessel Cooling Crystallizer," *J. Crystal Growth*, **13-14**, 500 (1972).
Randolph, A. D., and K. Rajagopal, "Direct Measurement of Crystal Nucleation Growth Rate in a Backmixed Crystal Slurry," *Ind. Eng. Chem. Fundamentals*, **9**, 165 (1970).
Shah, B. C., R. W. Rousseau, and W. L. McCabe, "Polyethylene vs. Stainless Steel Impellers for Crystallization Processes," *AIChE J.*, **19**, 194 (1973).
Strickland-Constable, R. F., "The Breeding of Crystal Nuclei—A Review of the Subject," *AIChE Symp. Ser. No. 121*, **68**, 1 (1972).
Sung, C. Y., J. Estrin, and G. R. Youngquist, "Secondary Nucleation by Fluid Shear," *AIChE J.*, **19**, 957 (1973).
Youngquist, G. R. and A. D. Randolph, "Secondary Nucleation in a Class II System: Ammonium Sulfate-Water," *AIChE J.*, **8**, 421 (1972).

Manuscript received October 16, 1974; revision received December 23, 1974 and accepted January 2, 1975.

Drag Reduction in Solid-Fluid Systems

I. RADIN
J. L. ZAKIN
and
G. K. PATTERSON

Department of Chemical Engineering
University of Missouri—Rolla
Rolla, Missouri 65401

Pressure drop measurements were made on a variety of dilute solid-liquid suspension systems in order to study the effects of particle shape and size, concentration, fluid viscosity, and tube diameter on friction factor. The central objective was to determine under what conditions drag reduction would occur.

SCOPE

There have been many conflicting reports on measurements of drag for the turbulent flow of dilute solid-liquid suspensions through pipes. Some have shown drag increases above the drag of the liquid at the same flow rate; some have shown little effect; some have shown drag lower than the drag of the liquid at the same flow rate; and some have been mistakenly described as showing decreased drag. The measurements reported here were made over a wide range of Reynolds numbers in a 6.3-mm and a 25.5-mm I.D. tube in order to determine when and if such decreased drag (drag reduction) occurs.

Spherical, platelet, and needle-shaped rigid particles (nonfibrous) of many types and sizes from submicron to 420 μm were used in a range of concentrations up to 4% by weight to determine their drag effect. Fibrous solids of uniform varieties, such as chopped nylon and rayon fibers, and nonuniform varieties, such as dispersed newsprint and asbestos, were extensively tested over the same concentration range.

CONCLUSIONS AND SIGNIFICANCE

Drag reduction could always be obtained with fibrous additives of l/d greater than 25 to 35 if the concentration was sufficiently high. The drag reduction behavior of these suspensions is different from that of high polymer and soap solutions. Laminar flow behavior is stabilized giving lower than normal friction factors and transition to turbulent flow extends over a range of up to two decades or more of Reynolds number. Four flow regions can be recognized. High l/d promotes drag reduction for a given d. Smaller diameter, more flexible fibers, are more effective at equal l/d values. No drag reduction was obtained with spherical, platelet, or needle-shaped rigid solid additives.

Concentration studies pointed up the need for measurements over a range of flow rates as the relative drag reducing abilities of different concentrations of additives vary with the flow region. The relative dispersing abilities of fluids of different viscosity apparently affect the drag reducing character of the suspensions more than viscosity.

Examination of solid-gas suspension data in the literature shows similar flow behavior. It is believed that electrostatic charges on the particles have a major effect on solid-gas friction factor behavior.

The drag ratio DR for conduit flow of an incompressible fluid-additive system is defined as

$$DR = \frac{(\Delta P/L)_{\text{fluid-additive}}}{(\Delta P/L)_{\text{fluid}}} \quad \overline{V} = \text{constant}$$

The fluid-additive system is said to be drag reducing if the drag ratio is less than unity. Drag reduction for steady flow

Correspondence concerning this paper should be addressed to J. L. Zakin. I. Radin is with Gulf Research and Development Company, Pittsburgh, Pennsylvania 15230.

in conduits has been observed only in turbulent flow or in extended laminar-turbulent transition regions. Reduced drag in turbulent flows past solid boundaries has also been observed. Practical applications of this phenomenon are in reduced pumping requirements in oil well fracturing operations and in fire fighting systems and in the external flow encountered in naval and other nautical systems.

Many high polymer and several soap solutions in both water and hydrocarbon solvents have been shown to be drag reducing (Patterson et al., 1969). In these systems it is generally agreed that drag reducing behavior is associated with the viscoelastic nature of the solutions which is caused by the high molecular weight polymer molecules or by the soap micelles in solution. They are effective in the shear region near the solid wall. Therefore, at a constant Reynolds number, the drag reducing effect of polymer or soap additives is reduced as the scale of the system is increased.

Since viscoelasticity and drag reduction for a fluid-additive system at any concentration are sensitive to polymer molecular weight or soap micelle aggregation number, mechanical and/or chemical degradation of the additive will decrease the drag reducing effectiveness of these types of systems. Degradation of high polymers is irreversible. Soap micelles are generally not as sensitive to mechanical degradation as high polymers. In aqueous systems where micelle degradation has occurred, the micelles reform immediately when shear stresses are lowered below a critical value (Savins, 1967). Degraded soap micelles in hydrocarbon solvents are slow to reform. However, in general, higher concentrations of soap are required than of high polymers and the latter have been preferred for practical applications.

Literature reports showing drag reduction in solid-fluid suspensions are not as clear as those in polymer and soap solutions. In many cases investigators were not looking for drag reducing behavior and in many others the data were not presented in a straightforward manner. Nevertheless, many fiber-liquid suspensions have been shown to be drag reducing and mechanical degradation is negligible for most of these additives. The literature on solid-gas suspensions is confusing. Seemingly similar systems exhibit drag ratios less than, equal to, and greater than unity in various investigations.

In the present work, the pressure drop behavior of suspensions of various shapes in tube flow was investigated to determine the critical variables affecting drag reduction. The effects of particle shape and size, fluid viscosity, and tube diameter were studied. Spherical, plate-like, and rigid needle-shaped low aspect ratio particles were tested as well as both natural and synthetic high aspect ratio flexible fibers in water, water-glycerine, and light mineral oil. Measurements were made in two tube sizes. In addition, a study was made of the solid-gas flow literature to determine what variable or variables in solid-gas systems might be responsible for the anomalous behavior of these systems, that is, in similar systems under similar flow conditions solid additives have been observed to give both drag reducing and drag increasing behavior. Similarities between the mechanisms in solid-liquid and solid-gas drag reducing flow behavior were also sought.

LITERATURE REVIEW

Solid-Liquid Suspensions

In the literature on pipe flow of solid suspensions in liquids there are two reports which claimed drag reduction for solids which did not have relatively large aspect ratios

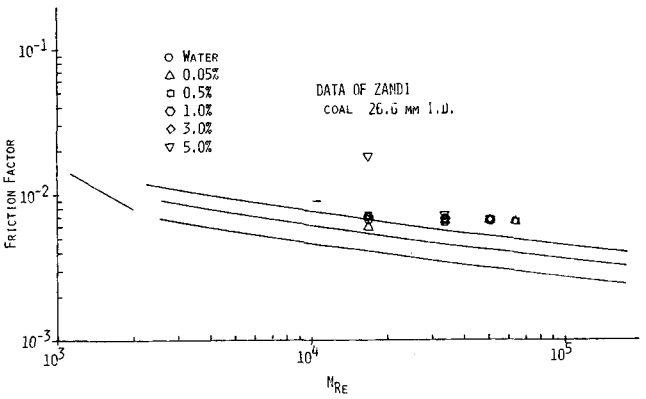

Fig. 1. Friction factor versus Reynolds number, 26.6-mm I.D., data of Zandi.

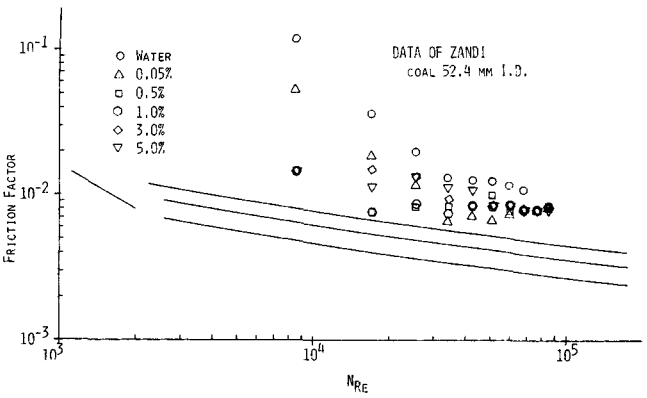

Fig. 2. Friction factor versus Reynolds number, 52.4-mm I.D., data of Zandi.

($l/d > 10$). In the first, a paper by Zandi (1967), pressure drops were measured in 15.8-, 20.9-, 26.6-, 40.9- and 52.4-mm I.D. pipes* at concentrations from 0.01% to 7.5% solids by weight. Materials tested were: coal 74-300 μm, fly ash < 150 μm, clay 210-840 μm, and activated charcoal < 45 μm.

Figures 1 and 2 are friction factor vs. water Reynolds number plots of data tabulated in Zandi's paper for coal in 26.6- and 52.4-mm pipes. The conventional laminar and van Karman curves, indicating the Fanning friction factor for Newtonian flow in smooth tubes are shown as solid lines, as well as lines indicating 20 and 40% drag reduction. Friction factors and Reynolds numbers were calculated using the properties of the suspending fluid. In this type of plot, drag reduction begins where the suspension friction factor points fall below the von Karman curve. These data are typical of his other suspensions. The exact pipe diameters, which were not reported, were assumed to be those for commercial Schedule 40 steel pipe. The results for pure water lie well above the predicted values for smooth tubes in all cases, suggesting that the pipe walls were rough. Inconsistencies in the suspension results are seen by observing the behavior of the most dilute (0.05%) coal suspension. For example, friction factors in the 15.8- and 26.6-mm pipes for this concentration are almost identical to those for pure water, while friction factors in the 20.9- and 32.4-mm pipes for the same suspension are considerably lower than those measured for water, although still above those predicted for smooth tubes. The differences in deviations from the von Karman curve

* Pipe sizes were reported as ½-, ¾-, 1-, 1½-, and 2-in. diameters.

for different pipes suggest differences in roughness and not differences in suspension behavior.

It is doubtful that drag reduction was actually observed in these experiments. The data are not self consistent and only a few of the lowest Reynolds number points fall below the curve predicted by the von Karman equation for smooth tubes. It may be that in some of the tubes, such as the 20.9 and 52.4-mm, pipe wall roughness was substantially reduced by the abrasive action of the solids after the pure water measurements were made.

In his thesis Pirih (1970) reported drag reduction with rigid particle suspensions in 15.8, 26.6, 40.9, 67.8, and 78-mm I.D. polyvinylchloride pipe. Pirih and Swanson (1972) described the 78-mm pipe as hydraulically smooth. The particles were a colloidal precipitate of rhombic crystals of milling yellow dye. The crystals, suspended in their mother liquor, were described as rigid and nonelastic with an aspect ratio of 5.7. The actual particle size was not known but was stated to be submicron. Particle size (but not aspect ratio) was increased by decreasing the suspension temperature.

It is not clear whether the drag reduction is caused by the presence of low concentrations, 0.17 to 0.23%, of the rigid precipitate or the higher concentrations, 0.53 to 0.47%, of the milling yellow in solution. Since all turbulent flow measurements were made at temperatures below the initial precipitation temperature, some of the nonprecipitated dye still in solution, but near precipitation, may have formed large agglomerates which caused the drag reduction. Some of the large effects on drag reduction that they reported for small changes in crystal length and concentration (due to solution temperature change) are more reasonably explained by changes in aggregation of molecules in solution. Similar behavior with micelles of soaps (Savins, 1967) and nonionic surfactants (Zakin and Chang, 1972) near their precipitation temperatures has been reported previously.

In addition, several authors (Bobkowicz and Gauvin, 1965; Hoyt, 1972; Vaseleski, 1973; Zandi, 1967) have claimed that nonfibrous solid-liquid suspension pipe flow pressure drop measurements of earlier authors indicated drag reduction. Those earlier papers which have been so described are the water suspensions of sand used by Blatch (1906), of emery used by Maude and Whitemore (1958), and of thoria used by Thomas (1962) and by Eissenberg (1964). However, examination of the data presented in these papers shows that none of these nonfibrous suspensions was drag reducing over any significant range of flow rates, nor did Blatch, Maude and Whitemore, Thomas or Eissenberg claim them to be drag reducing. Only in a narrow transition range do a few pressure drop points appear to be drag reducing. The confusion over the results of the last three papers may have been caused by their friction factor-Reynolds number plots in which the suspension density was used to calculate the friction factor. These high suspension densities gave low friction factors, but not drag reduction, since drag reduction is defined as occurring only when the wall shear stress is below that of the suspending fluid alone. In addition, suspension viscosity terms which were greater than the viscosity of water were used by Thomas and Eissenberg in the calculation of the Reynolds number.

In contrast to the investigations of nonfibrous suspensions, many investigators, particularly in the paper industry, have noted significant drag reduction in fiber-water suspensions. Some of these results are included in Table 7. One of the earliest reports was by Forrest and Grierson (1931). Representative of more recent work are papers by Robertson and Mason (1957), Daily and Bugliarello (1961), and Mih and Parker (1967), who measured pressure drops in tubes ranging in size from 1.905- to 10.15-cm I.D., using for the most part wood fibers. All three papers noted the existence of three more or less distinct regions.* Friction factor measurements (shown in Figure 3) using a 2% rayon fiber-water suspension in our own apparatus illustrate these regions:

1. The first region which occurs at low Reynolds numbers is called the *plug flow region.* In this region a plug of fibers was visually observed to be surrounded by a fiber-free annulus of fluid in laminar flow (Robertson and Mason, 1957). On a friction factor versus suspending fluid Reynolds number plot this region is characterized by a straight line with a slope steeper than -1 lying to the right (higher Reynolds numbers) of the laminar curve for the suspending fluid and extending to or somewhat beyond the intersection with the von Karman line. This is equivalent to shear thinning behavior. In this plug flow region the friction factor for any type of fiber is a function of bulk velocity, tube diameter, and fiber concentration. At the same fluid Reynolds number, either an increase in concentration or a decrease in velocity will cause the friction factor to increase.

2. The second region is referred to as the *mixed flow region.* In this region the fluid in the annulus was observed to become turbulent (Mih and Parker, 1967; Robertson and Mason, 1957) and the plug begins to disintegrate in the high shear region at the annulus-plug interface. With increasing bulk velocity the plug diameter becomes smaller. The friction factor still decreases with increasing Reynolds number but at a rate slower than in the plug flow region but faster than for a Newtonian fluid in turbulent flow in a smooth pipe.

3. The third region is called the *fully turbulent region.* In this region the friction factor is not decreasing as rapidly with increasing Reynolds number as a pure fluid and in many cases the friction factor is increasing with Reynolds number. The data of investigators using synthetic fiber drag reducing additives (Bobkowicz and Gauvin, 1965; Kerekes and Douglas, 1972) follow the same trends on plots of this type.

Comparison of Drag Reduction in Solid-Gas Suspensions with That in Fiber-Liquid Suspensions

Drag reduction in solid-gas systems has been claimed by the original authors or by later authors in papers listed in Table 1. Several other solid-gas transport studies using similar flow systems and variables but which were not drag reducing are listed in Table 2.

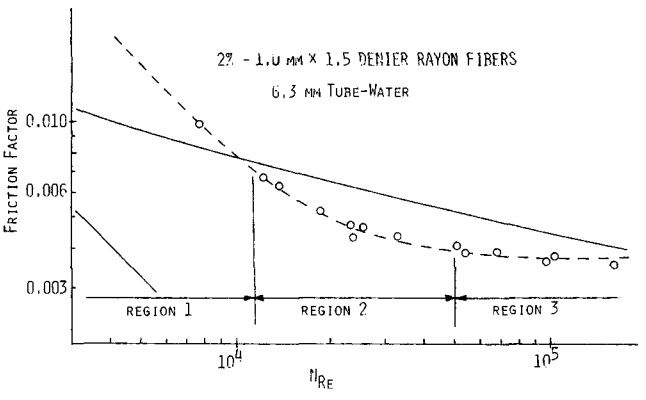

Fig. 3. Friction factor versus Reynolds number, 2% — 1.0 mm × 1.5 denier rayon.

* These regions were observed directly and indirectly by visual, photographic, and velocity profile observations.

In Tables 1 and 2 it can be seen that over wide ranges of the variables of particle size, pipe size, particle diameter to pipe diameter ratio, loading ratio and Reynolds number, both drag reducing and nondrag reducing behavior have been observed. Thus, there is apparently at least one important variable which is not accounted for by the

TABLE 1. GAS-SOLID STUDIES IN WHICH DRAG REDUCTION WAS OBSERVED OR CLAIMED

Author	Particle material	Particle size	Flow direction	Pipe material and I.D. mm		Loading ratio kg_{solid}/kg_{gas}	Reynolds number range	Maximum drag reduction	Comments
Boothroyd	Zinc	8-20 μm	Vert.	Brass	25.4 50.8 76.2	0-25	35,000-100,000	25% in 50.8 & 76.2; 75% in 25.4 mm	Large amount of scatter in data. Probable errors in correcting for pressure drop due to solid accel.
Boothroyd & Mason	Alumina	15 μm 40 μm 70 μm	Vert.	Perspex	25.4 50.8 76.2	0-6	50,000-180,000	25.4 mm 45% 50.8 mm 15% 76.2 mm 35%	Friction factor essentially independent of particle size and loading ratio in 25.4 mm tube.
Soo & Trezek	M_gO	36 μm	Horiz.	Brass	127	0-3	130,000-295,000	Very small or none	Pure air data appears to be incorrect.
Peters & Klinzing	Glass beads	25 μm 50 μm	Vert.	Copper	25.4	0-1.6	14,000 20,000 27,000	Less than 10% (only) with 25 μm at 14,000	Incorrectly assumed he had eliminated charge effects.
Boyce & Blick	Silica dust Glass beads	2-60 μm 100 μm 200 μm 840 μm 1,680 μm	Not stated	Plexiglas	69.9	0-2.8	9,000-63,000	25% 2-60 μm 10% 1,680 μm Based on air data	Pure air data is 8% high in mid Reynolds number range. Pipe might have downward slope.
Rosetti & Pfeffer	Glass beads	10 μm 20 μm 25 μm 34 μm 59 μm	Horiz. and Vert.	Stainless Pyrex	22.2 25.4	0-2	13,000-27,000	20% with small beads in horiz. 70% with larger beads in vertical	Values of loading ratios in doubt. May have insufficient entrance length.
Kane, Weinbaum & Pfeffer	Glass beads	15 μm 21 μm 21.6 μm 36 μm 55 μm	Horiz and Vert.	Stainless	22.2	Most 0-1 Some 0-3	12,000-25,000	40% with 36 μm & 55 μm in vert.; 10% with smaller particles in both horiz. and vert. Large part. gave drag increase in horiz.	Part size effect on pressure drop opposite to that of Boyce & Blick.
Sproull	Limestone dust 40% < 10 μm Talc 99% < 10 μm			Concentric Cylinder Viscometer		0.05 and 0.20	Taylor number about 60	Claimed viscosity reduction of 10 to 40%	Incorrect viscosity reduction claim.

TABLE 2. GAS-SOLID SUSPENSION STUDIES IN WHICH NO DRAG REDUCTION WAS OBSERVED

Author	Particle material	Particle size	Flow direction	Pipe material and I.D. mm		Loading ratio kg_{solid}/kg_{gas}	Reynolds number range	Comments
Vogt and White	Sand	200μm 325 μm	Horiz. & vert.	Iron	15.8	0-35	9,000-39,000	Pipe I.D. 15.8 mm, large pressure taps (10.3 mm O.D.).
Belden and Kassel	Catalyst	950 μm	Vert.	Steel	12.0 26.0	0-14	3,360-22,600	At low flow rates negative pressure drops due to over correction for static head.
Mehta, Smith and Comings	Glass beads	36 μm 97 μm	Vert.	Iron	15.8	0-15	2,900-26,000	First used glass test section, had visible electrostatic discharges.
Farber	Al_2O_3-SiO_3 Catalyst	10-220 μm	Horiz. & vert.	Glass	17.0	0-16	15,000-45,000	
Richardson and McLeman	Coal Perspex Polystyrene Lead Brass Aluminum M_gO_2	500-760 μm 760 & 1,525 μm 350 μm 305 μm 380 μm 230 μm 760 μm	Horiz.	Brass	25.4	0-15	35,000-85,000	Observed electrostatic charging with polystyrene, M_gO_2 and Perspex. In some cases the pressure drop increased with time, in some it decreased, but never obtained drag reduction.
Kramer and DePew	Glass beads	62 μm 200 μm	Vert.	Glass	12.7 19.1 25.4	0-5	5,670-50,000	Did not report his own pressure drop data. Pressure drop correlation based on velocity profile data measurements did not predict drag reduction.
Reddy and Pei	Glass beads	100 μm 150 μm 200 μm 270 μm	Vert.	Copper	100.1	0-.6	55,000-100,000	Inside of system had antistatic coating.
Duckworth and Chan	Glass Ballotini	125 μm 350 μm	Horiz.	Copper	31.5	0-8	25,000-50,000	Incorrectly assumed elimination of charge effect by use of 40 millicurie polonium source.
McCarthy and Olson	Calcium carbonate Glass beads Lucite beads	2-6 μm 65 μm 230 μm	Horiz.	Glass	25.4	0-.6	10^5-10^6	High Reynolds number so gas accelerates along Fanno line. They based f_{susp} on ρ_{susp} leading later authors to believe they observed drag reduction.
Zenz	Glass beads Salt	575 μm 88-250 μm	Horiz. & vert.	Lucite	44.5	0.75-70	4,000-32,000	
Trezek and France	Glass beads	110 μm 200 μm	Horiz.	Copper Copper Stainless	19.1 15.9 6.4	0-4	40,000 in 6.4 130,000 in 19.1	Choked flow, no drag reduction, errors in friction factor.
Hariu and Molstad	Sand Sand Catalyst	270 μm 210 μm 108 μm	Vert.	Glass	6.8 13.5	.7-50	1,500-9,000	
Duckworth and Kakka	Glass Ballotini	40 μm 85 μm 105 μm 340 μm 670 μm 1,270 μm	Horiz & vert.	Copper	31.8	0-7	20,000-80,000	Drag ratio decreased with increasing N_{Re} at a constant loading ratio. At a constant Reynolds number, drag ratio increased with particle size (for glass Ballotini) in copper pipe, independent of particle size in glass pipe.
			Horiz.	Glass	25.4			
	Lead	400 μm 570 μm 650 μm						
	Polystyrene	700 μm						

above properties but which causes gross differences in the flow behavior.

No obvious differences in the flow systems of those papers reporting drag reduction and those which do not are apparent. Drag reduction was observed in systems with electrically conducting [brass (Boothroyd, 1966), copper (Peters and Klinzing, 1972) and stainless (Kane et al., 1973)] and nonconducting [pyrex (Rosetti and Pfeffer, 1972) and Plexiglas (Boyce and Blick, 1970; Boothroyd and Mason, (1971)] test sections. Likewise results showing no drag reduction were obtained in both conducting [steel (Mehta et al., 1957; Vogt and White, 1948) and brass (Richardson and McLeman, 1960)] and nonconducting [glass (Farber, 1949; Kramer and Depew, 1972; McCarthy and Olson, 1968) and lucite (Zenz, 1948)] test sections. The same can be said of particle electrical properties, that is, both conducting and nonconducting particles have been observed to be drag reducing and not drag reducing. Thus, the existence of drag reduction does not appear to depend on either the electrical characteristics of the test section alone or on the electrical characteristics of the particles alone, but possibly depends on the electrostatic charge caused by the particle-wall and particle-particle contact, giving rise to particle-particle and particle-wall forces.

Friction factor-gas Reynolds number plots for some drag reducing solid-gas suspensions resemble those for fiber-liquid suspensions. The data in Figure 4 (Kane et al., 1973; Rosetti and Pfeffer, 1972) show Region 2 (left side) and Region 3 (right side) behavior, and the data in Figure 5 (Mason and Boothroyd, 1971) show Region 1 behavior. These figures indicate the importance of electrostatic charge as a variable in these systems.

The data shown in Figure 4 were taken with nominal 30-μm glass beads in a system whose vertical test section had been changed from 25.5-mm I.D. pyrex glass (left side) to 22.2-mm I.D. stainless steel (right side). It appears that in both cases drag reduction occurred due to a delayed and extended transition from laminar to turbulent flow. However, in the glass tube the flow at 12,000 to 22,000 Reynolds number is on the laminar side of transition while in the metal tube it is on the turbulent side in the same Reynolds number range. In the glass tube, the electrostatic forces are apparently stronger and have a greater effect on flow conditions. If data were taken at higher Reynolds numbers in the glass tube, it is likely that the friction factor would return to the von Karman line as the metal tube data do.

In Figure 5 (Boothroyd and Mason, 1971) the pressure

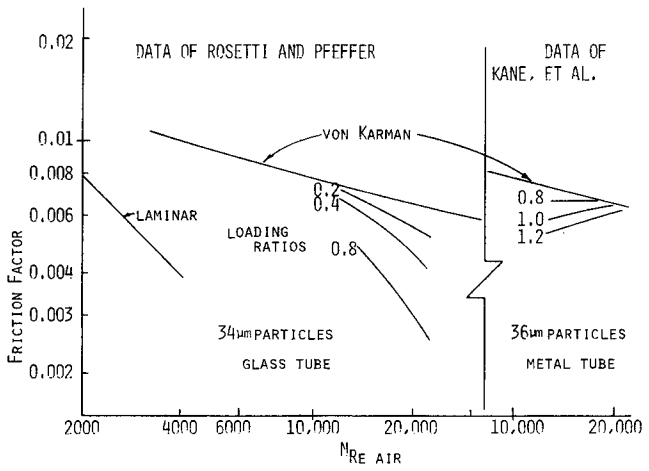

Fig. 4. Friction factor versus Reynolds number, data of Rosetti and Pfeffer and Kane et al.

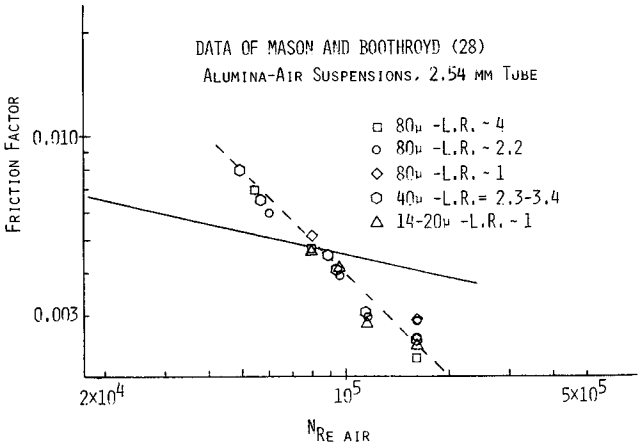

Fig. 5. Friction factor versus Reynolds number, data of Boothroyd.

drop in the 25.4-mm I.D. tube is little affected by particle size and loading ratio (within the particle size and loading ratio ranges reported). The slope of the friction factor versus air Reynolds number results is close to that of laminar flow but displaced to air Reynolds numbers about two orders of magnitude greater than those normally associated with laminar flow. Mason and Boothroyd's (1971) and Boothroyd's (1966) data in a 50.8-mm I.D. tube with the same particles is quite different with almost no observed drag reduction except at low loading ratios and with the smallest particles. Presumably, charge effects are less significant in the larger tube. Some of the latter data are at wall stresses at which drag reduction was observed in the 25.4 mm tube. Similar results are obtained when the data of Boyce and Blick (1970) are plotted as friction factor versus air Reynolds number for various loading ratios. Regions 1 and 2 behavior can be seen with the laminar region moving to higher air Reynolds numbers as the loading ratio is increased.

One can speculate that drag reduction in gas-solid suspensions is due to a delayed and extended laminar-to-turbulent transition region probably caused by electrostatic forces which have the effect of inhibiting particle and fluid motion and hence stabilizing viscous behavior and giving a large apparent increase in viscosity. At some high Reynolds number in the extended transition region, inertial forces begin to dominate electrostatic forces and eventually the flow returns to apparently normal turbulent behavior. The electrostatic forces are analogous to interparticle effects obtained in fiber-liquid suspensions.

In similar systems exhibiting drag increasing behavior, the pressure increase may be due to charged particles adhering to the tube wall and increasing its roughness. Drag increasing behavior in the absence of charge may be due to the increased density of the fluid caused by the addition of solids. Authors (Duckworth and Chan, 1973; Peters and Klinzing, 1972) who have tried to eliminate the effect of particle charge by ionizing the suspending air probably failed to ionize a significant number of air molecules (Radin, 1974).

Effects of particle charge do not seem important in solid-liquid suspensions, probably because of the large viscous forces involved (also in water charges are dissipated rapidly because of the water's conductivity).

EXPERIMENT

Pressure drops were measured in two recirculating systems. The smaller had a 6.3-mm I.D. test section and the larger had a 25.5-mm I.D. test section. The systems and experimental procedures used in making measurements are described below.

Small Unit Description and Procedures

Figure 6 is a schematic of the small unit. The test section was constructed of a 1.02-m length of nominal 6.3-mm I.D. stainless steel tubing. Pressure drop measurements were made across two 152.4-mm test sections beginning 100 and 124 diameters downstream from the tube entrance. Pressure taps were carefully bored with a #72 drill (0.632 mm). A length of unhardened drill rod about 0.006-mm in diameter less than the test section I.D. was inserted into the test section to serve as a backup when drilling the pressure tap holes and thus avoid any burrs on the inner walls of the test section. Figure 6 also shows details of the pressure tap connections. The test section was vertical. To avoid vibration it was isolated from the rest of the system by short pieces of Tygon tubing connected at either end.

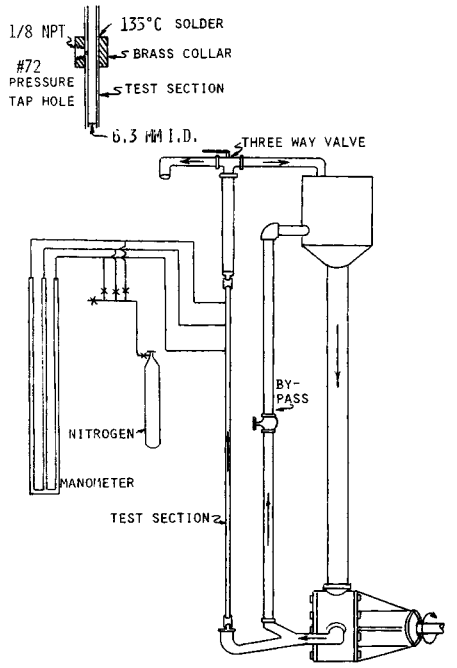

Fig. 6. Small unit schematic.

A Viking gear pump (Model K124), driven by a 1500 W, 325 rev/min gear-head motor, was used to provide flow rates up to about 5×10^{-4} m^3/s. This flow rate corresponds to a Reynolds number of about 180,000 based on the viscosity and density of water. No temperature control was provided, but both the viscosity and the density of the suspending fluid were corrected for temperature in calculating Reynolds numbers and friction factors. The temperature was measured immediately downstream of the test section. Pressure indicators were fluid manometers. Nitrogen separated the process fluid from the manometer fluid. For high pressures the manometer fluid was mercury and for low pressures either water or Meriam oil (S.G. = 2.95). In most cases the system held about 40 kg of process fluid.

The measured friction factors for pure fluid agreed with the von Karman equation for smooth tubes over the range of flow rates run to within about ±5% (maximum).

Large Unit Description and Procedures

Figure 7 is a schematic of the large unit. The test sections were constructed of 3.05 meter lengths of nominal 25.4-mm I.D. stainless steel tubing. Pressure drop measurements were made across a 0.457 m test section beginning 85 diameters from the tube entrance. The pressure taps were bored with a #72 drill and then the entire length of each of the tubes was honed to eliminate any irregularities or burrs and to ensure that they were hydraulically smooth.

A Peerless centrifugal pump (Model CLO 2 × 1 × 8½)

Table 3. Nonfibrous Solids Tested

Solid material	Fluid	Particleshape	Particle size	Concentration, %
Alumdum (aluminum oxide)[a]	Oil	Approx. spherical	38 μm (est.)	0.1, 0.75
Degussa colloidal aluminum oxide[b]	Oil	Spherical	0.005-0.030 μm (ultimate)	0.1, 0.5
Cabosil M-5 (colloidal silica)[c]	Oil	Spherical	0.012 μm (ultimate)	0.1, 0.5
	Water	Spherical	0.012 μm (ultimate)	.75
Cabosil H-5 (colloidal silica)[c]	Oil	Spherical	0.007 μm (ultimate)	0.1, 0.5
	Water	Spherical	0.007 μm (ultimate)	0.1, 0.5, 1.0 1.0, 2.0, 4.0
Glass beads[d]	Oil	Spherical	44-88 μm	0.1, 1.0
	Water	Spherical	44-88 μm	0.5, 1.0, 3.0
	Oil	Spherical	88-149 μm	0.1, 1.0
	Water	Spherical	88-149 μm	0.5, 3.0
	Oil	Spherical	297-420 μm	0.1, 1.0
Englehardt Attaclay (attapulgite derivative)[e]	Water	Approx. spherical agglomerates (needle-like ultimate particles l/d ≈ 15)	18 μm	0.5, 1.0, 2.0, 4.0
Englehardt Attasorb RVM (attapulgite derivative)[e]	Water	Approx. spherical agglomerates (needle-like ultimate particles l/d ≈ 15)	2.9 μm	0.5, 1.0, 2.0, 4.0
Englehardt Attagel 50 (attapulgite derivative)[e]	Water	Approx. spherical agglomerates (needle-like ultimate particles l/d ≈ 15)	0.14 μm	0.5, 1.0, 2.0, 4.0
Georgia Kaolin Thixo-Jell #3 (bentonite derivative)[f]	Water	Platelets	Not available	1, 2, 4

[a] Edmund Scientific, Barrington, New Jersey.
[b] Degussa, Inc., Kearny, New Jersey.
[c] Cabot Corporation, Boston, Massachusetts.
[d] Zero Manufacturing Company, Washington, Missouri.
[e] Englehardt Minerals and Chemical Company, Minerals and Chemicals Division, Edison, New Jersey.
[f] Georgia Kaolin Company, Elizabeth, New Jersey.

was driven at 3100 rpm by a 15,000 W motor to provide flow rates up to about 6.3×10^{-3} m³/s. This flow rate corresponds to a Reynolds number of about 394,000 based on the viscosity and density of water. Temperature was maintained at 30°C ± 0.1°C by means of cooling coils mounted in the tank. Pressure drop measurements were made with manometers. For high pressures the manometer fluid was Meriam fluid with a specific gravity of 2.95 and for low pressures Meriam fluid with a specific gravity of 1.20. With both manometers the pressure tap lines were allowed to fill with water so that the effective specific gravity of the fluids was 1.95 and 0.20, respectively. The system held about 210 kg of process fluid.

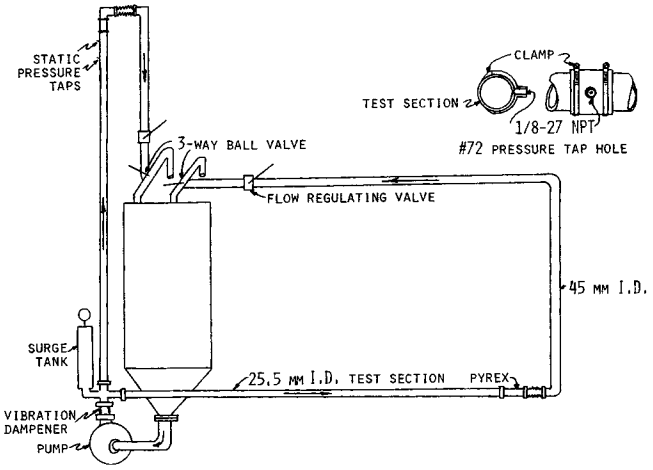

Fig. 7. Large unit schematic.

Pure water friction factors were about 10% too high when compared with the von Karman equation for smooth tubes. The reason for high pressure drops is not clear. Pipe or pressure tap roughness is unlikely as the tubes were honed smooth. Other possibilities are insufficient entrance length ($L/D = 85$) for fully developed turbulent flow and a slight amount of cavitation in the pump causing slight pressure pulses in the test section. Since the data were repeatable and since comparisons between additive and nonadditive systems were of primary interest, the high values were accepted. Drag ratios were, however, always calculated using the predicted value of the friction factor (calculated with the von Karman equation).

From repeated runs with water, the small unit results were repeatable to better than ±3% and the large unit results to about ± 5%. Repeatability for suspension flows depended on the suspension characteristics, some of which changed with time, but a reasonable figure for the small unit in most cases was about ± 5%. Not enough data were repeated in the large unit to make a reasonable estimate.

Suspensions Studied

Tables 3, 4, and 5 list the various suspensions for which friction factors were measured. In most cases the following technique was used to prepare a suspension for testing in either unit. While the suspending fluid was circulating, the proper amount of solid was slowly added to the fluid. The suspension was then allowed to circulate for several hours to allow complete dispersion of the solid. The required pressure drop measurements were then made as described above.

TABLE 4. CHARACTERIZED FIBROUS SOLIDS TESTED IN WATER

Solid material	Nominal length, mm	Nominal diameter, Denier	Nominal diameter, mm	Nominal l/d	Concentration, %	Max. drag reduction, %
Nylon fibers*	0.5	1.5	0.014	37	0.5	2
	0.5	1.5	0.014	37	1.0	7
	0.5	1.5	0.014	37	2.0	13
	1.0	1.5	0.014	74	0.2	2
	1.0	1.5	0.014	74	1.0	13
	1.0	1.5	0.014	74	2.2	17
	1.0	6.0	0.028	37	0.5	4
	1.0	6.0	0.028	37	1.0	3
	1.0	6.0	0.028	37	2.0	7
	1.0	6.0	0.028	37	4.0	20
	2.0	3.0	0.019	105	1.0	12
	2.0	6.0	0.028	74	0.5	?
	2.0	6.0	0.028	74	1.0	5
	2.0	6.0	0.028	74	2.0	13
Rayon fibers*	0.5	1.5	0.012	43	0.2	none
	0.5	1.5	0.012	43	1.0	5
	0.5	1.5	0.012	43	2.0	15
	0.5	1.5	0.012	43	3.0	23
	1.0	1.5	0.012	86	0.2	2
	1.0	1.5	0.012	86	1.0	17
	1.0	1.5	0.012	86	2.0	25
	1.0	1.5	0.012	86	3.0	25+
	1.0	5.5	0.023	45	0.2	none
	1.0	5.5	0.023	45	1.0	3
	1.0	5.5	0.023	45	2.0	12
	2.0	5.5	0.023	90	0.5	2
	2.0	5.5	0.023	90	1.0	10
	2.0	5.5	0.023	90	2.0	15
	2.0	5.5	0.023	90	2.9	22
Cotton fibers*	0.5-0.75			25-35**	0.2	none
	0.5-0.75			25-35**	1.0	none
	0.5-0.75			25-35**	2.0	5
	0.5-0.75			25-35**	3.0	20
				25-35**		

All above fibers tested in 6.3-mm I.D. tube.
* Obtained from Microfibers, Inc., Pawtucket, R. I.
** Measured wet.

Table 5. Additional Fibrous Solids Tested

Solid material	Particle size and l/d	Fluid and tube I.D., mm	Concentration, %
Fybex, potassium titanate*	Diameter 0.10-0.16 μm, l/d 40:1	Water—6.3	½, 1, 2, 4
SG-144, asbestos**	l/d 10^2-10^3	Water—6.3	1, 2, 3
T-135 0, asbestos**	l/d 10^2-10^3	Water—6.3	1, 2, 3
SG-210, asbestos**	Diameter .025 μm, l/d 10^2-10^3	Water—6.3	1, 2, 3
Newsprint		Water—6.3	½, 1.1, 2
		Water—25.5	½, 1
HPO, asbestos**	Diameter .025 μm, l/d 10^2-10^3	Water—6.3	½, 1, 2
RG-444[1] asbestos**	Diameter ≈ .025 μm, l/d 10^2-10^3	Water—6.3	¾
		Oil—6.3	¾, 1, 2
		Oil + ¼% water—6.3	2
7T02, asbestos***	Diameter ≈ .02 μm, l/d 10^2-10^3	Water—6.3	¾, 1½
7M05, asbestos***	Diameter ≈ 0.02 μm, l/d 10^2-10^3	Water—6.3	¾
		Water—glycerine—6.3	¾
4T04, asbestos***	Diameter ≈ 0.02 μm, l/d 10^2-10^3	Water—6.3	¼, ¾
		Water + 0.1% surfynol 104—6.3	¼
		Water—glycerine—6.3	¾
7M02, asbestos***	Diameter ≈ 0.02 μm, l/d 10^2-10^3	Water—6.3	¾, 1½
4T30, asbestos***	Diameter ≈ 0.02 μm, l/d 10^2-10^3	Water—6.3	⅛, ¼, ¾
		Water—25.5	¼, ¾
		Water + ¼% Aerosol OT—6.3	¼
		Water + 0.01% Aerosol OT—6.3	⅛
		Water + 0.01% Aerosol OT + 0.1% Surfynol 104—6.3	⅛
4T30, asbestos***	Diameter ≈ 0.02 μm, l/d 10^2-10^3	Water + 0.05 Surfynol 104—6.3	¾
		Water—glycerine—6.3	¾
		Oil—6.3	¼, ¾
		Oil + ¼% water—6.3	¾
3T12 asbestos***	Diameter 0.02 μm, l/d 10^2-10^3	Water—6.3	¼, ¾
		Water—25.5	¼, ¾
Turner Brothers,[2] asbestos****	$l/d > 10^4$	Water—6.3	25, 50, 100, 250 500 wppm

(1) Chrysotile asbestos which has been rendered hyprophobic by surface modification.
(2) Contained 1 part Aerosol OT per 2 parts asbestos.
* E. I. du Pont de Nemours & Co., Wilmington, Delaware.
** Union Carbide Corp., Niagara Falls, New York.
*** Canadian Johns-Manville Co., Ltd., Asbestos, P. Q., Canada.
**** Turner Brothers Asbestos Co., Ltd., Rochdale, England.

RESULTS AND DISCUSSION

Effect of Particle Shape

Nonfibrous Solids. The shapes, sizes, and concentrations of all nonfibrous (spherical, elongated, and plate-like) particles tested are listed in Table 3. Equivalent diameters ranged from 0.005 to 0.03 μm to 297 to 420 μm and concentrations from 0.1 to 4.0% by weight. All suspensions of the nonfibrous solids were tested for drag reduction in the 6.3-mm tube. In this extensive experimental study of nonfibrous solids, none of them showed drag reduction at any concentration or Reynolds number tested. This is in agreement with most previous reports in the literature for solid-liquid suspensions as discussed in the Literature Review.

It appears, therefore, that it is unlikely that drag reduction caused by nonfibrous solids suspended in liquids exists, except for short transition regions.

Fibrous Solids. At a concentration above some minimum value for each fiber, all of the flexible fiber suspensions showed drag reducing behavior. Drag reduction is greatest near the junction of Regions 2 and 3. At higher flow rates drag reduction decreased. In some cases, particularly in the 25.5-mm I.D. test section, the pressure drop approached that of the pure fluid at the highest flow rates, indicating the possibility of a fourth region where the friction factor is essentially that of the suspending Newtonian fluid.

Bobkowicz and Gauvin (1965) studied the effects of suspensions of drag reducing nylon fibers of various sizes and shapes. They observed that drag reduction increased with the aspect ratio (l/d) of the fibers at a fixed concentration. Our results in Table 4 for rayon and nylon fibers, which could be characterized, confirm their findings. However, these results show that for fibers of approximately equal aspect ratios, drag reducing ability increased with a decrease in fiber diameter, a result also shown by their data, although they did not note it.*

This may be due to the larger number of fibers present at a given concentration with the attendant increase in interparticle contacts or it may be due to increased fiber flexibility. An example of the small but significant differences in drag reducing ability of rayon fibers of essentially equal aspect ratios but different fiber diameters is shown in Figure 8.

* For example, at equal aspect ratios of 26, their nominal 0.5 mm by 3 denier (actual 0.52 mm by 0.0202 mm) nylon fiber gave drag ratios from 5 to 40% lower than their nominal 1.25 mm by 15 denier (actual 1.21 mm by 0.457 mm) nylon, depending on Reynolds number and concentration.

Each asbestos sample studied was too varied in fiber shape and size to be characterized simply. However, at the lower concentrations, the longer fibered samples were superior to the shorter fibered. The extremely long fibered Turner Brothers asbestos gave the best drag reduction of all the fibers tested at concentrations an order of magnitude or more below those of the other fibers. However, these fibers rapidly degraded in the 6.3-mm system in which they were tested, making it difficult to complete a full run without degradation. The long fibered Johns Manville 3T12 and 4T30 were the most effective stable samples tested at low concentrations (¼%). At higher concentrations comparisons of results for different fibers are not as clear.

Relative Effectiveness of Fiber Materials

Only the nylon, rayon, and cotton fibers studied were uniform enough to be characterized unambiguously. Comparison of pressure drop results at equal concentrations and nearly equal fiber diameters and aspect ratios shows that the rayon fibers are perhaps a little more effective as drag reducers than the nylon fibers (Table 4).

Asbestos and paper fiber suspensions exhibited greater extensions of the laminar friction line and hence greater drag reduction at equal concentrations than the nylon and rayon fibers. This can be attributed in part to high aspect ratios, but probably more to the irregular fiber surfaces and much higher flexibilities, which might cause greater tendency to entangle giving stronger fiber networks compared to those formed by the synthetic fibers. Table 6 lists the fibers tested in order of increasing effectiveness and the concentration required for about 15 to 25% drag reduction in the 6.3 mm tube.

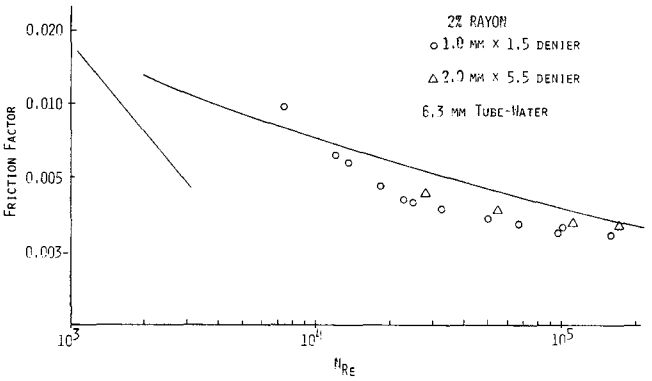

Fig. 8. Friction factor versus Reynolds number, effect of fiber diameter.

TABLE 6. EFFECTIVENESS OF DRAG REDUCING FIBERS

Fiber		Concentration required in water for 15 to 25% D.R. in 6.3-mm tube
Cotton		3%
Potassium titanate		4%
Nylon Rayon	low l/d, large d	3%
Nylon Ravon	large l/d, small d	1½-2½%
SG-144 T 135 0 SG-210 Newsprint HPO RG-444 7T02 7M05 4T04 7M02 4T30 3T12		1-1½%
Turner Brothers		¼-¾%
		500 wppm

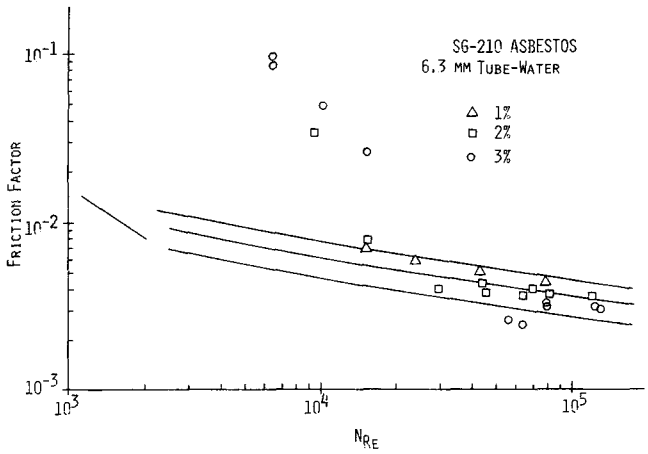

Fig. 9. Friction factor versus Reynolds number, effect of fiber concentration.

Effect of Concentration

At low concentrations, the fibers have little effect on apparent suspension viscosity or drag reduction. As concentration and, therefore, particle-particle interactions increase, drag reduction at a fixed flow rate goes through a maximum. At still higher concentrations and hence higher apparent suspension viscosities, the flow appears to become laminar (actually plug flow) and pressure drop increases rapidly. However, these high concentration suspensions show excellent drag reducing ability at higher flow rates. These effects are illustrated by friction factor vs. water Reynolds number data shown in Figure 9 for SG 210.

Frequently pressure drop data for drag reducing suspensions have been reported on plots other than the friction factor-suspending fluid Reynolds number plot described above. In some instances this has complicated the interpretation of the data.

For instance, a friction factor vs. suspending fluid Reynolds number plot clarifies the unusual concentration effects reported by Kerekes and Douglas (1972) for suspensions of nylon fibers. They noted an apparent optimum concentration for drag reduction from comparisons of their results at different concentrations at a number of fixed flow rates. Thus, at each fixed flow rate they reported that for low nylon concentrations there was little drag reduction. However, as concentration increased, drag reduction became significant and increased with concentration up to a relatively high concentration, where pressure drops rose rapidly with further increase in concentration. Their data for 1.016 mm × 3 denier nylon fibers are shown in Figure 10 as friction factor vs. water Reynolds number.

Kerekes and Douglas' data cover only a narrow water Reynolds number region, but portions of the regions shown in Figure 3 can be seen at each concentration. Their 0.49% suspension results are close to their pure water results. As concentration increased to 1.95%, the last portion of Region 3 and the start of Region 4 are observed. At 3.70%, the suspension is in Region 3 while at 4.63% it appears to be in the final portion of Region 2. The 5.37% suspension is quite thick and at low velocities is in plug flow (Region 1). It enters Region 2 at higher velocities and becomes drag reducing. If the results are examined

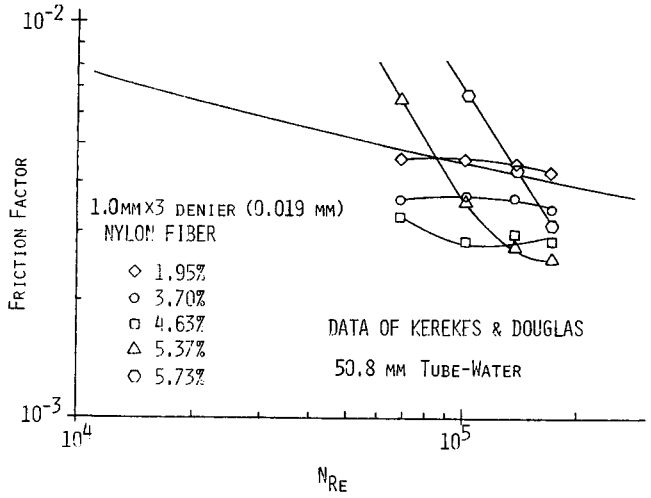

Fig. 10. Friction factor versus Reynolds number, data of Kerekes and Douglas.

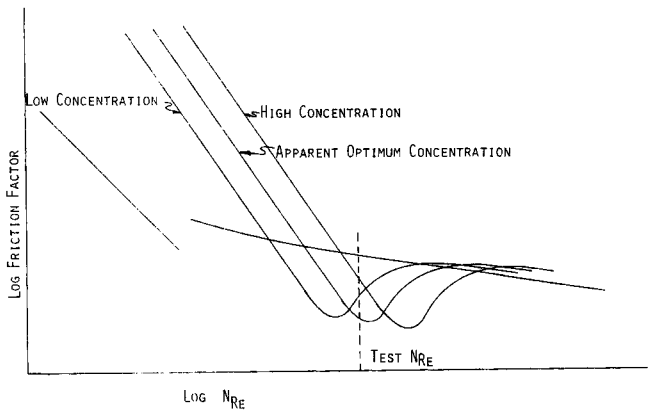

Fig. 11. Friction factor versus Reynolds number, idealized to show concentration effect.

at their lowest velocity (1.22 m/s), there appears to be a sharp loss of drag reducing ability above 4.63%. In reality this is merely a reflection of the viscous nature of the 5.37% suspension which is in plug flow at this velocity in this tube. At the highest velocity (3.05 m/s), this concentration gave the most drag reduction. Further increase in concentration to 5.73% and 5.94% gave predominantly plug flow behavior even at higher velocities. Presumably, at still higher flow rates these two high concentration suspensions would demonstrate typical Region 2, 3 and 4 behavior.

The steep concentration peaks for maximum drag reduction observed by Arranaga (1970) for Avitene H and to a lesser extent for Avicel CM dispersions at a fixed solvent Reynolds number probably result from these same phenomena. Figure 11 is an idealized friction factor-fluid Reynolds number plot of a non-Newtonian fluid which exhibits drag reduction only in a very narrow laminar-turbulent transition region. If pressure drop measurements were made at the Reynolds number indicated it would appear that drag reduction occurred, the magnitude of which depended on the concentration. Thus the results of Arranaga and others showing concentration dependent drag reduction at a single flow rate may be misinterpreted if it is not recognized that they hold only for a particular velocity. Had data been obtained over a wider range of Reynolds numbers, curves similar to these (Figure 11) might have been obtained.

Thus it is clear that since drag reduction in solid-liquid suspensions is a result of a greatly extended laminar-turbulent transition region, great care needs to be taken in interpreting pressure drop data for narrow flow rate ranges as there is no certainty in which flow regime the measurements are being made.

Effect of Fluid Viscosity

Asbestos suspensions were tested in three suspending fluid systems: water, water-glycerine (3.2×10^{-3} N·s/m² at 32°C) and mineral oil (3.6×10^{-3} N·s/m² at 32°C). Figure 12 is a friction factor-pure suspending fluid Reynolds number plot of ¾% 4T30 suspended in these fluids in the 6.3-mm I.D. tube.

At equal concentrations, the mineral oil system gave the least drag reduction at all turbulent Reynolds numbers, while the water-glycerine mixture gave the most. It is possible that the glycerine acted as a dispersant or as a bridge between particle contacts which enhanced the stabilizing effect of the asbestos and improved its drag reducing ability. The mineral oil, which does not wet asbestos well, is least effective as a dispersant or as a bridging agent for asbestos, and the poorer drag reduction obtained reflects this. Figure 12 also has some data points showing the effect when ¼% water was added to the oil. Apparently the water further reduced the interaction between the asbestos and the oil and drag reduction was lost.

Effect of Tube Diameter

The effect of tube diameter was studied using the same suspensions in 6.3-mm and 25.5-mm I.D. tubes. Figure 13 is a friction factor-water Reynolds number plot for ¼%

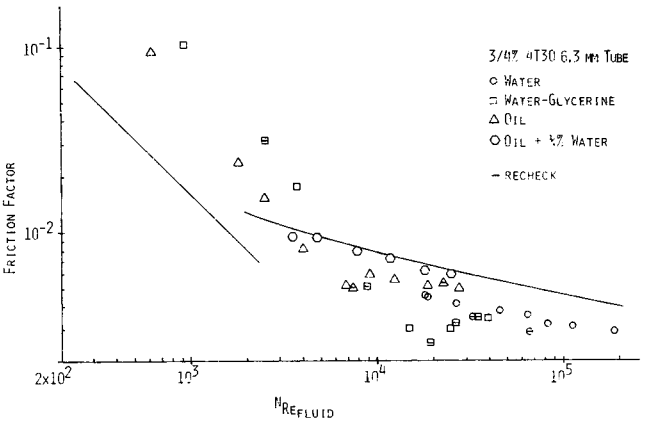

Fig. 12. Friction factor versus Reynolds number, effect of suspending fluid viscosity.

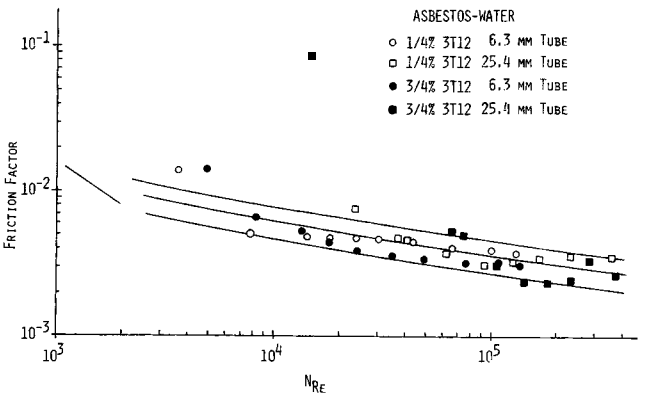

Fig. 13. Friction factor versus Reynolds number, effect of tube diameter, 3T12.

and ¾% 3T12 asbestos-water suspensions in these tubes.

At a concentration of ¼%, the suspension in the 6.3-mm tube gave a slightly greater maximum drag reduction. However, at ¾% the situation was reversed and lower drag ratios were obtained in the 25.5-mm tube. In the former case this may be due to the fact that the fiber size is an appreciable fraction of the tube diameter, thus limiting fiber mobility and hence strengthening the fiber network. In the latter case the higher concentration overwhelms the fiber size to tube diameter considerations. Due to the fact that in Region 2 flow, where minimum drag ratios occur, a larger tube has a greater percentage of its flow in a nonshear (plug) condition, it might be expected that larger tubes will give lower minimum drag ratios than smaller tubes. Lower minimum friction factors in their large versus their small tubes were also noted by Daily and Bugliarello (1961) and Mih and Parker (1967) for all of their suspensions. However, their smallest diameter tubes were 19.1 and 50.8 mm, respectively.

The clear water annulus near the wall probably explains data obtained by Lee et al. (1974), showing that the combined effect of fiber and polymer on drag reduction was greater than the sum of the polymer effect and the fiber effect. The addition of the fibers effectively reduced the characteristic length of the system since the shear (velocity gradient) region was confined to the clear water annulus. Thus, the effectiveness of the polymer additive is enhanced, as it is most effective in regions of large velocity gradients which prevail in the annulus region near the wall in fiber suspension flow. This would not only explain the synergistic effect of the two additives but would also explain the decreased effect of tube diameter on the drag reduction of these combined systems which they observed, as the annulus thickness might not vary much with tube diameter. This hypothesis on the importance of the annulus region for these mixed systems is also supported by the fact that they noted that degraded polymers were still effective when fibers were present. It has been noted (Ellis, 1970) that degraded polymers, which are ineffective in larger diameter tubes, are still effective in small diameter tubes where high shear stresses and velocity gradients exist.

It was noted from suspension data for 3T12 and data of other investigators that there might be a correlation between the velocities where the plug flow (Region 1) line crossed the von Karman line for a particular fiber at a given concentration for different tube diameters.

At this crossover point,

$$f_{\text{turb}} = f_{\text{susp}}$$

$$f_{\text{turb}} \simeq \frac{0.046}{(N_{Re})^{0.2}} \simeq \frac{\tau_w}{\rho V^2/2\, g_c}$$

where $0.046(N_{Re})^{0.2}$ is an approximation to the von Karman friction factor line. For Region 1 (plug) flow a good assumption is that all of the velocity gradient occurs in the clear fluid annulus and the velocity at the inner edge of the annulus is approximately the bulk mean velocity $\overline{V}$. Therefore

$$\tau_w = \mu_{\text{water}}\, (dV/dy)_{\text{wall}}$$

and

$$(dV/dy)_{\text{wall}} = \overline{V}/D_{\text{annulus}}$$

therefore

$$\mu_{\text{water}}\overline{V}\cdot 2\cdot g_c/\rho\overline{V}^2 D_{\text{annulus}} = 0.046/(N_{Re})^{0.2}$$

or

$$(N_{Re})^{0.2}/\overline{V} = 0.046\, \rho\, D_{\text{annulus}}/2\, g_c\, \mu_{\text{water}}$$

If, at the von Karman crossover, D_{annulus} is primarily a function of the fiber and its concentration and nearly independent of tube diameter, then $(N_{Re})^{0.2}/\overline{V}$ should be constant at the von Karman crossover for any tube size.

Table 7 is a tabulation of $(N_{Re})^{0.2}/\overline{V}$ for data of investigators who have reported pressure drops in Region 1 for various tube diameters. Guthrie (1958) reported only n' and K', so the velocities where his friction factors crossed the von Karman line were calculated from these values.

The results are inconclusive. Guthrie's kraft fibers do not correlate well; however, his sulfite fibers do. Mih and Parker's (1957) rayon and kraft fibers correlate with the exception of their 1% kraft for which Region 1 flow data deviated from a straight line before crossing the von Karman line. Daily and Bugliarello's (1961) data for their wood pulps give fair correlation, but their nylon fiber results are erratic.

Due to difficulties in obtaining low enough flow rates in the 6.3-mm tube to obtain Region 1 behavior in the present investigation, only data for the 3T12 asbestos-water suspensions can be checked. The ¼% data correlate, but as can be noted in Table 7 the ¾% data give poor results. Since these data were obtained in two independent systems and different suspensions had to be prepared for each system, slight differences in concentration at the higher concentration or in asbestos dispersion could cause relatively large differences in the suspensions' apparent viscosities. The other investigators all ran the same suspensions in their different sized test sections which were in parallel.

The clear fluid annulus model explains why Ellis (1970) required higher concentrations of asbestos in a smaller diameter tube than in a larger diameter tube to achieve the same drag reduction when pressure drops were measured at the same water Reynolds number in each tube.

Effect of Dispersants

Two surface active agents were used in an attempt to aid in the dispersion of the asbestos fibers in water. They were Aerosol OT-75% (75% surfactant, 20% water, 5% alcohol) and Surfynol 104, which is also a defoamant. The former was used by Hoyt (1970) and Lee et al. (1974) to disperse all their asbestos suspensions. Using Aerosol OT, foaming problems were encountered. Figure 14 indicates that ¼% 4T30 gave a much lower drag ratio when ¼% Aerosol OT was added. However, before the run was completed (run from low to high flow rates), air entrainment caused a given weight of suspension to approximately double in volume. This reduced the drag reducing effect as can be noted from the recheck points on this figure.

Pressure drop measurement of suspensions of ⅛% 4T30, ⅛% 4T30 with 0.01% Aerosol OT, and ⅛% 4T30 with 0.01% Aerosol OT and 0.1% Surfynol 104 were also compared. Very little difference in pressure drop results was observed. Foaming occurred in all mixtures which contained Aerosol OT. However, with 0.01% Aerosol OT most of the foaming appeared to be near the liquid surface rather than throughout the suspension as occurred with the ¼% 4T30 plus ¼% Aerosol OT mixture.

This foam appeared to float much of the asbestos to the surface of the fluid, thus effectively removing it from suspension and resulting in a loss of drag reducing behavior. The addition of 0.1% Surfynol 104, which is a defoamer as well as surfactant, did not change the visual appearance of the foaming suspension or the pressure drop results.

Pressure drop results in the 6.3-mm tube with ¼% 4T04 asbestos suspended in water were not influenced by the presence of 0.1% Surfynol 104. In a ¾% 4T30 asbestos-water suspension run in the 25.5-mm tube, the addition of 0.05% Surfynol 104 also had no effect on the pressure drop of the suspension. The addition of Surfynol

TABLE 7. TEST OF TUBE DIAMETER CORRELATION

Author	Tube diameter, mm	Material	Concentration, %	Canadian Standard freeness,[1] ml	$\frac{K' \times 10^3}{N \cdot S^{n'}}$ m^2	n'	Velocity at von Karman cross-over, m/s	Water Reynolds number at von Karman cross-over	$\frac{Re^{0.2}}{\overline{V}}$ s/m	Error based on smaller tube, %
Mih and Parker	50.8	Rayon	0.2				0.30	18,000	23.66	
	101.6						0.39	48,000	22.14	−6.4
	50.8	Rayon	0.5				0.62	38,000	13.29	
	101.6						0.81	98,000	12.30	−7.5
	50.8	Hardwood Kraft	0.5	630			0.37	22,500	20.06	
	101.6						0.43	52,000	20.40	+1.7
	50.8	Hardwood Kraft	1.0	630			0.91	55,000	9.75[2]	
	101.6						0.81	98,000	12.30[2]	+26.1
Daily and Bugliarello	19.1	Nylon	0.25				0.20	4,000	26.27	
	50.8						0.50	27,500	15.45	−41.2
	19.1	Nylon	0.5				0.68	14,000	9.92	
	50.8						0.64	35,000	12.67[2]	+27.7
	19.1	Long Lac 17	0.5				0.46	9,400	13.55	
	50.8						0.58	31,500	13.68[2]	+1.0
	19.1	Long Lac 17	1.0				0.93	19,000	7.71[2]	
	50.8						1.09	60,000	8.28[2]	+7.4
	19.1	Cossa River 55	0.5				0.39	8,000	15.47	
	50.8						0.44	24,000	17.08[2]	+10.4
	19.1	Groundwood					0.33	6,800	17.70	
	50.8	Poplar	0.5				0.35	19,100	20.52	+15.9
	19.1	Groundwood					0.49	10,000	12.88	
	50.8	Poplar	0.75				0.60	33,000	13.35	+3.7
	19.1	Groundwood					0.90	18,500	7.93	
	50.8	Poplar	1.0				0.89	49,000	9.74	+22.9
Radin	6.3	3T12[3] As-					0.66	4,800	8.25	
	25.5	bestos	0.25				0.97	30,600	8.14	−1.4
	6.3	3T12[3] As-					0.93	6,995	6.32	
	25.5	bestos	0.75				2.17	68,600	4.27	−32.4
Guthrie	12.7	Bleached Kraft			7.18	1.0	0.78	10,630	8.19	
	25.4	softwood	0.55	410	6.70	1.0	0.61	16,700	11.46	+39.9
	12.7	Bleached Kraft			25.38	0.80	1.22	16,700	5.73	
	25.4	softwood	0.93	620	36.39	0.78	1.06	28,800	7.35	+28.4
	12.7	Bleached Kraft			81.40	0.62	1.19	16,220	5.34	
	25.4	softwood	1.37	620	83.79	0.60	0.88	24,100	8.55	+46.4
	12.7	Bleached Kraft			8.62	0.95	1.10	15,080	6.23	
	25.4	softwood	0.43	670	9.10	0.92	0.53	14,500	12.82	+105.8
	12.7	Bleached Kraft			17.72	0.85	1.18	16,160	5.89	
	25.4	softwood	0.80	670	21.07	0.86	0.97	26,400	7.90	+34.1
	12.7	Bleached Kraft			81.40	0.70	1.96	26,750	3.92	
	25.4	softwood	1.19	670	88.58	0.68	1.41	38,500	5.86	+49.5
	12.7	Bleached sulfite			4.60	0.99	0.68	9,290	9.14	
	25.4	softwood	0.5	375	23.94	0.82	0.87	23,650	8.61	−5.7
	12.7	Bleached sulfite			718.2	0.40	2.03	27,700	3.81	
	25.4	softwood	1.95	375	718.2	0.45	2.41	65,750	3.82	+0.1
	12.7	Bleached sulfite			4.79	1.00	0.78	10,620	8.19	
	25.4	softwood	0.5	390	22.02	0.85	0.95	26,100	8.05	−1.8
	12.7	Bleached sulfite			62.24	0.70	1.52	20,800	4.81	
	25.4	softwood	1.1	390	102.94	0.69	1.73	47,100	4.97	+3.4

[1] A measure of how quickly water will drain from pulp. The greater freeness, the faster water will drain.
[2] Data deviated from straight line before crossing von Karman line, extension of linear portion of laminar line used for calculations.
[3] Data for each tube taken with fresh suspensions.

104 did not cause any foaming problems.

The effect of either dispersant, without any asbestos present, on the pressure drop of water was not checked. However, other investigators (Ellis, 1970; Hoyt, 1972; Lee et al., 1974) have reported that the addition of Aerosol OT has no significant effect on friction factors of water.

Comparison of Fiber-Liquid Friction Factors with Those Obtained for Polymer and Soap Solutions

The shape of the friction factor-Reynolds number curves for drag reducing fibrous solid suspensions in liquids is different from those observed with polymer or soap solutions. The differences for several types of drag reduction in which friction factors gradually deviate from an extension of the laminar line are illustrated by the idealized curves shown in Figure 15. In this schematic, all fluids are taken to have the same apparent n' and K' rheological characteristics. Curve A is typical of fiber-liquid suspensions showing Regions 1, 2, and 3 behavior. No degradation was observed with any of the fiber-liquid systems (with the exception of the Turner Brothers asbestos) and both low and high flow rate results could be repeated after

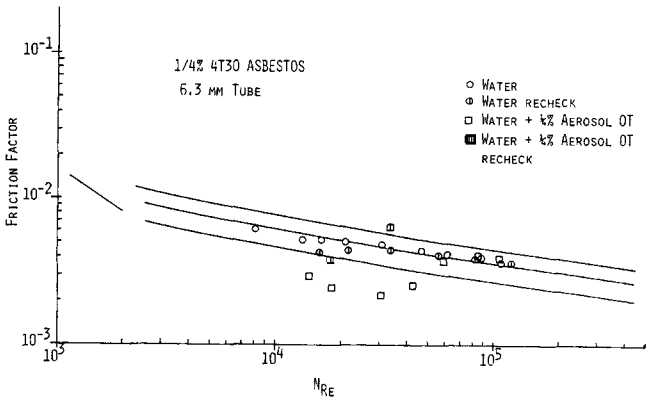

Fig. 14. Friction factor versus Reynolds number, effect of dispersant, 1/4% 4T30.

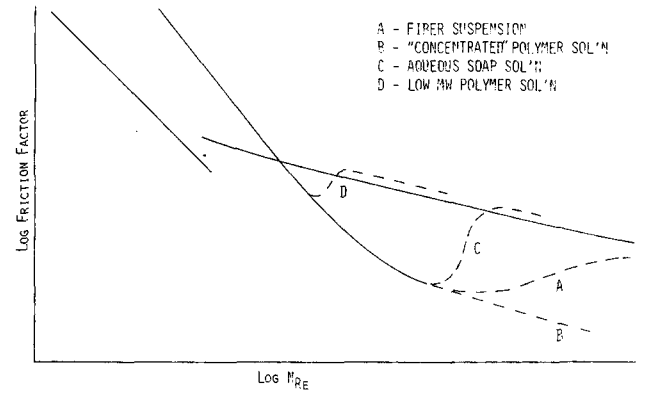

Fig. 15. Friction factor versus Reynolds number, idealized types of drag reducing behavior.

high flow rate measurements were made (assuming the suspension was well dispersed). In concentrated polymer solutions (Curve B), friction factor data gradually deviate from an extension of the laminar line (Liaw et al., 1971). There is no decrease in drag reduction at high flow rates unless the polymer is physically degraded in which case the low flow rate results are not repeatable. In aqueous soap solutions (Savins, 1967) there is also a gradual deviation from an extension of the laminar line but above some critical wall shear stress, soap micelles are mechanically broken up and friction factors rise steeply to the von Karman line or above it (Curve C). The micelles reform at low wall shear stresses and the results at any flow rate can be repeated. Hershey and Zakin (1967) also described drag reducing results for a few polymers which gave a short extension of the laminar region due to flow stabilization, followed by a normal transition and by nondrag reducing turbulent behavior (Curve D). Low flow rate results were repeatable.

Tentative Mechanism for Drag Reduction in Fiber-Liquid Suspensions

Drag reduction in fiber-liquid suspensions is believed to be due to the presence of an entangled fiber network. The strength of this network, on which drag reduction depends, is a function of fiber concentration, length, diameter, flexibility, surface properties, moisture retention, and fiber conformation. At low Reynolds numbers this network causes the fluid in the core of the tube to move as a plug. The fluid near the tube wall is relatively fiber free, and it is in this annular region where the velocity gradient is large. The displacement to higher water Reynolds numbers of the laminar line is caused by the higher than normal (laminar flow) shear rate in this annular region. As the flow rate is increased the diameter of the fiber plug decreases due to the increasing shear stress at the plug-annulus interface. This increase in annulus gap causes the slope of the laminar line to be steeper than -1 and gives the apparent non-Newtonian nature of the suspension.

A tentative proposal for the existence of fiber-liquid drag reduction is that the velocity profile in the critical turbulence generation region ($5 < y^+ < 30$) is less steep at the end of region 1 with fibers present than the velocity profile of the pure liquid in turbulent flow at the same flow rate (Figure 16). Therefore the pressure drop is decreased. As the flow rate is further increased, the fluid in the annulus becomes turbulent. Because the plug diameter continues to decrease, the pressure drop does not increase as rapidly as predicted by the von Karman equation. This is Region 2 behavior. Eventually, due to the turbulence in the annulus, the plug diameter decreases rapidly, probably disappearing in Region 3 as the friction factor approaches the von Karman line.

ACKNOWLEDGMENT

Acknowledgment is made to the donors of the Petroleum Research Fund, administered by the American Chemical Society, for support of this research.

NOTATION

D = diameter, tube
$D_{annulus}$ = annulus thickness
d = diameter, particle
f = fanning friction factor, $\tau_w/\rho\overline{V}^2/2g_c$
g_c = gravitational constant
K' = defined by $D\Delta P/4L = K'(8\overline{V}/D)^{n'}$ for laminar flow
L = length, tube
l = length, particle
N_{Re} = Reynolds number $\rho D\overline{V}/\mu$

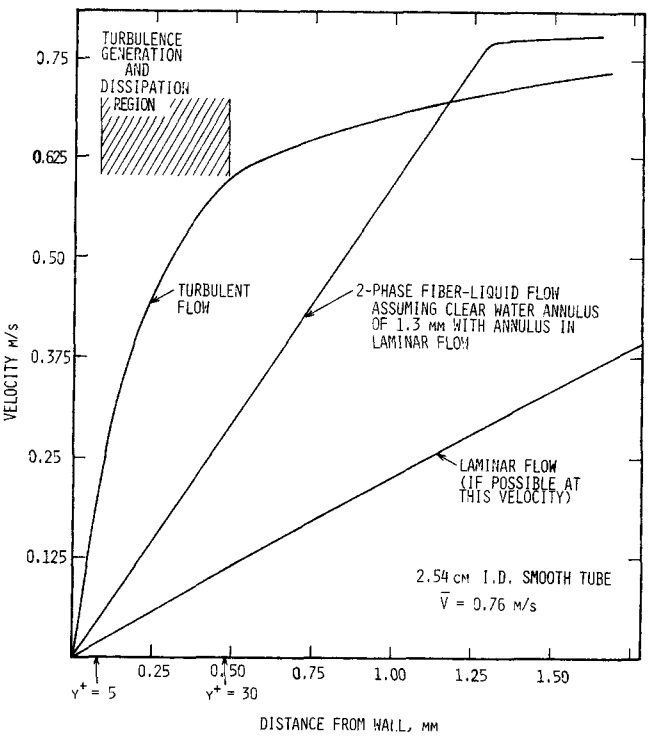

Fig. 16. Velocity profile for fiber suspension.

n' defined by $D\Delta P/4L = K'(8\overline{V}/D)^{n'}$ for laminar flow
P = pressure drop in axial direction for conduit flow
V = velocity
$\overline{V}$ = bulk (average) velocity
y = distance from tube wall
y^+ = dimensionless distance from tube wall,

$$y^+ = y\sqrt{\frac{\tau_w \rho}{\mu}}$$

ρ = density
τ_w = wall shear stress (for tube flow) = $D\Delta P/4L$
μ = Newtonian viscosity

LITERATURE CITED

Arranaga, A. B., "Friction Reduction Characteristics of Fibrous and Colloidal Substances," *Nature*, **225**, 447 (1970).

Belden, D. H., and L. S. Kassel, "Pressure Drops Encountered in Conveying Particles of Large Diameter in Vertical Transfer Lines," *Ind. Eng. Chem.*, **41**, 1174 (1949).

Blatch, N. S., "Discussion: Water Filtration at Washington, D.C., *Trans. ASCE*, **57**, 400 (1906).

Bobkowicz, A. J., and W. H. Gauvin, "The Turbulent Flow Characteristics of Model Fiber Solutions," *Can. J. Chem. Eng.*, **43**, 87 (1965).

Boothroyd, R. G., "Pressure Drop in Duct Flow of Gaseous Suspensions of Fine Particles," *Trans. Instn. Chem. Engrs.*, **44**, T306 (1966).

Boothroyd, R. G., and J. J. Mason, "Comparison of Friction Factors in Pneumatically Conveyed Suspensions Using Different Sized Particles in Pipes of Varying Size," *Proc. Pneumotransport 1*, Cambridge, England, C1-1 (1971).

Boyce, M. P., and E. F. Blick, "Fluid Flow Phenomena in Dusty Air," *Trans. ASME, J. Basic Eng.*, **D92**, 495 (1970).

Daily, J. W., and G. Bugliarello, "Basic Data for Dilute Fiber Suspensions in Uniform Flow with Shear," *Tappi*, **44**, 497 (1961).

Duckworth, R. A., and T. K. Chan, "The Influence of Electrostatic Charges on the Pressure Gradient During Pneumatic Transport," *Proc. Pneumotransport 2*, Cambridge, England, A5-59 (1973).

Duckworth, R. A., and R. S. Kakka, "The Influence of Particle Size on the Frictional Pressure Drops Caused by the Flow of a Solid-Gas Suspension in a Pipe," *Proc. Pneumotransport 1*, Cambridge, England, C3-29 (1971).

Eissenberg, D. M., "Measurement and Correlation of Turbulent Friction Factors of Thoria Suspensions at Elevated Temperatures," *AIChE J.*, **10**, 403 (1964).

Ellis, H. D., "Effects of Shear Treatment on Drag-Reducing Polymer Solutions and Fibre Suspensions," *Nature*, **226**, 352 (1970).

Farber L., "Flow Characteristics of Solid-Gas Mixtures in a Horizontal and Vertical Circular Conduit," *Ind. Eng. Chem.*, **41**, 1184 (1949).

Forrest, F., and G. A. H. Grierson, "Friction Losses in Cast Iron Pipe Carrying Paper Stock," *Paper Trade J.*, **298** (May 28, 1931).

Guthrie, W. E., "An Apparent Viscosity for Use in the Application of Reynolds Numbers to the Flow of Dilute Pulp Suspensions," *Tappi*, **42**, 232 (1959).

Hariu, O. H., and M. C. Molstad, "Pressure Drop in Vertical Tubes in Transport of Solid by Gases," *Ind. Eng. Chem.*, **41**, 1148 (1949).

Hershey, H. C., and J. L. Zakin, "Existence of Two Types of Drag Reduction in Pipe Flow of Dilute Polymer Solutions," *Ind. Eng. Chem. Fundamentals*, **6**, 381 (1967).

Hoyt, J. W., "Turbulent Flow of Drag Reducing Suspensions," Naval Undersea Center TP 299, San Diego, Calif. (July, 1972).

Kane, R. S., S. Weinbaum, and R. Pfeffer, "Characteristics of Dilute Gas-Solid Suspensions in Drag Reducing Flow," Paper presented at Pneumotransport 2, (1973).

Kerekes, R. J. E., and W. J. M. Douglas, "Viscosity Properties of Suspensions at the Limiting Conditions for Turbulent Drag Reduction," *Can. J. Chem. Eng.*, **50**, 228 (1972).

Kramer, T. J., and C. A. DePew, "Experimentally Determined Mean Flow Characteristics of Gas-Solid Suspensions," *Trans. ASME, J. Basic Eng.*, **D94**, 492 (1972).

DePew, C. A., "Heat Transfer to Flowing Gas-Solids Mixtures in a Vertical Circular Duct," Ph.D. thesis, Univ. California, UCRL-9280 (1960).

Lee, W. K., R. C. Vaseleski, and A. B. Metzner, "Turbulent Drag Reduction in Polymeric Solutions Containing Suspended Fibers," *AIChE J.*, **20**, 128 (1974).

Liaw, G. C., J. L. Zakin, and G. K. Patterson, "Effects of Molecular Characteristics of Polymers on Drag Reduction," *ibid.*, **17**, 391 (1971).

Maude, A. D., and R. L. Whitemore, "The Turbulent Flow of Suspension in Tubes," *Trans. Inst. Chem. Engrs.*, **36**, 296 (1958).

McCarthy, H. E., and J. H. Olson, "Turbulent Flow of Gas-Solid Suspensions," *Ind. Eng. Chem. Fundamentals*, **7**, 471 (1968).

Mehta, N. C., J. M. Smith, and E. W. Comings, "Pressure Drop in Air-Solid Flow Systems," *Ind. Eng. Chem.*, **49**, 986 (1957).

Mih, W., and J. Parker, "Velocity Profile Measurements and a Phenomenological Description of Turbulent Fiber Suspension Pipe Flow," *Tappi*, **50**, 237 (1967).

Patterson, G. K., J. L. Zakin, and J. M. Rodriguez, "Drag Reduction: Polymer Solutions, Soap Solutions and Particle Suspensions in Pipe Flow," *Ind. Eng. Chem.*, **61**, 22 (1969).

Peters, L. K., and G. E. Klinzing, "Friction in Turbulent Flow of Solid-Gas Systems," *Can. J. Chem. Eng.*, **50**, 441 (1972).

Peyser, P., "The Drag Reduction of Chrysotile Asbestos Dispersions," *J. Appl. Polymer Sci.*, **17**, 421 (1973).

Pirih, R. J., "Drag Reduction and Turbulence Structure Modification in the Turbulent Pipe Flow of Fractional Percent Colloidal Suspensions," Ph.D. thesis, Washington Univ., St. Louis, Missouri (1970).

———., and W. M. Swanson, "Drag Reduction and Turbulence Modification in Rigid Particle Suspensions," *Can. J. Chem. Eng.*, **50**, 221 (1972).

Radin, I., "Solid-Fluid Drag Reduction," Ph.D. thesis, Univ. Missouri-Rolla (1974).

Reddy, K. V. S., and D. C. T. Pei, "Particle Dynamics in Solids-Gas Flow in a Vertical Pipe," *Ind. Eng. Chem. Fundamentals*, **8**, 490 (1969).

Richardson, J. F., and M. McLeman, "Pneumatic Conveying Part II: Solids Velocities and Pressure Gradients in a One-inch Horizontal Pipe," *Trans. Instn. Chem. Engrs.*, **38**, 257 (1960).

Robertson, A. A., and S. G. Mason, "The Fow Characteristics of Dilute Fiber Suspensions," *Tappi*, **40**, 326 (1957).

Rosetti, J. J., and R. Pfeffer, "Drag Reduction in Dilute Flowing Gas-Solid Suspensions," *AIChE J.*, **18**, 31 (1972).

Savins, J. G., "A Stress-Controlled Drag-Reduction Phenomenon," *Rheol. Acta*, **6**, 323 (1967).

Soo, S. G., and G. J. Trezek, "Turbulent Pipe Flow of Magnesia Particles in Air," *Ind. Eng. Chem. Fundamentals*, **5**, 388 (1966).

Sproull, W. T., "Viscosity of Dusty Gases," *Nature*, **190**, 976 (1961).

Thomas, D. G., "Transport Characteristics of Suspensions: IV. Friction Loss of Concentrated-Flocculated Suspensions in Turbulent Flow," *AIChE J.*, **8**, 266 (1962).

Trezek, G. J., and D. M. France, "Axial Pressure Correlation for Accelerating Particulate Pipe Flow," *Ind. Eng. Chem. Fundamentals*, **7**, 247 (1968).

Vaseleski, R. C., "Drag Reduction in the Turbulent Flow of Fiber Suspensions," M.S. thesis, Univ. Delaware, Newark (1973).

Vogt, E. G., and R. R. White, "Friction in the Flow of Suspensions, Granular Solids in Gases Through Pipe," *Ind. Eng. Chem.*, **40**, 1731 (1948).

Zakin, J. L., and J. L. Chang, "Non-Ionic Surfactants as Drag Reducing Additives," *Nature Phys. Sci.*, **239**, 26 (1972).

Zandi, I., "Decreased Head Losses in Raw Water Conduits," *J. Am. Waterworks Assoc.*, **59**, 213 (1967).

Zenz, F. A., "Two-Phase Fluid Solid Flow," *Ind. Eng. Chem.*, **41**, 2801 (1948).

Manuscript received August 27, 1974; revision received November 26 and accepted November 29, 1974.